Full-image acquisition and analysis of hot heavy rail incorporating multiple CCD

Zengzhen Mi[a,*], Hongming Zhang[a], Jing Tang[a], Xingyuan Xu[a]
[a]College of Mechanical Engineering, Chongqing University of Technology, No. 69, Hongguang Avenue, Chongqing 400054, China.

ABSTRACT

The rail transportation industry is moving towards heavy loads, high speeds as well as high density operation, which places higher demands on the quality of heavy rail. The quality inspection of rail defects using machine vision first requires obtaining clear surface/planar images of multiple surfaces of the hot heavy rail. Therefore, a vision inspection solution is proposed, which uses a 6-lane linear CCD to photograph the tread surface, bottom surface, and upper and lower waist surfaces of the heavy rail. A comprehensive comparison of various types of light sources was conducted through experiments on chromaticity, brightness, and spectral power. To solve the problem of image overexposure due to infrared radiation of the hot heavy rail, the spectral radiation characteristics of the hot heavy rail were analyzed, and the imaging effects of adding different filters were compared and analyzed. Finally, to solve the problem of out-of-focus due to oscillation of the heavy rail during rolling, the image is analyzed by an automatic focus search strategy, and the results are fed back to the camera to achieve automatic focus, thus adaptively obtaining good image quality and laying a good foundation for further defects detection.

Keywords : Heavy rail, multi-sensor fusion, image acquisition, linear CCD, Clarity evaluation

1. INTRODUCTION

In recent years, China's railroad construction has achieved rapid development, by the end of 2022, the national railroad mileage reached 155,000 kilometers, including 42,000 kilometers of high-speed rail, ranking first in the world, heavy load and high-speed of rail is an inevitable trend, so the surface quality of heavy rail requirements are increasingly high. As a means of transportation for high-speed rail operation, the quality of heavy rail is an significant condition to ensure the safe transportation of railroads. In addition to the more stringent material, processing technology, geometric size and physical and chemical properties, surface defects have become an significant technical indicator [1-3].

Take a rail beam factory's heavy rail defects manual inspection method as an example, the traditional 100m heavy rail inspection line has 3 teams, each team is responsible for one-third of the length of the inspection, each team of 4 people, respectively, to inspect each side of the heavy rail. When the heavy rail moves to UF exit at high speed, the running speed is reduced to about 1 m/s. The inspectors irradiate to the surface of the heavy rail with strong light source through the gap of the baffle, and judge whether there are defects such as scratches and rolling scars according to the light reflection of the surface and experience. When any person finds a certain area with suspected defects, it will make the heavy rail stop running for further observation, then let the rail back and make it slow (when the suspected defects are found the heavy rail has crossed the inspector). Because the manual detection of defects require the rail running speed is not higher than 0.5 m / s, in order to be able to clearly identify the suspected defects are true defects, the forward speed of the heavy rail shall not be higher than 0.5 m / s, so that the detection speed is greatly reduced [4-5]. Manual visual inspection method of the heavy rail detection process is shown in Figure 1.

*mizengzhen@163.com

Seventh International Conference on Mechatronics and Intelligent Robotics (ICMIR 2023), edited by Srikanta Patnaik, Tao Shen, Proc. of SPIE Vol. 12779, 127792B · © 2023 SPIE · 0277-786X · Published under a Creative Commons Attribution CC-BY 3.0 License · doi: 10.1117/12.2688729

Figure 1. Manual visual method for the detection of defects on the upper and lower surfaces of heavy rails

NDT methods commonly used in industry can be divided into five major categories: radiation detection method, liquid penetration detection method, eddy current detection method, leakage magnetic detection method, ultrasonic detection method, machine vision detection method, etc [6-14]. Machine vision-based surface defects detection with machine vision, image pattern classification of the two major technologies as the core, has become mainstream in many industries in the detection of surface defects have been applied, and received wide attention from scholars at home and abroad, a comparison of the characteristics of different detection technologies are shown in Table 1.

Table 1. Comparative analysis of the characteristics of different detection techniques

Detection methods	**Advantages**	**Disadvantages**
Manual visualization	Greater flexibility, no need for expensive testing instruments	Poor real-time performance, low resolution, easy to miss and false detection
Stroboflash	Lower cost and reduced labor intensity of inspectors	Low degree of automation and low reliability of detection
Radioactive	Higher detection resolution, easier to judge the size and nature of defects	High cost, long detection period, radiation is harmful to humans
Liquid permeation	Simple equipment, display defects intuitive, can display all kinds of defects at the same time	The operation process is complicated, and only the defects exposed on the surface can be inspected
Eddy current	Can detect high-temperature object surface and sub-surface defects without coupling agent, fast detection speed	Some parameters of the measured object may interfere with the identification of defects
Magnetic leakage	Detects both minor defects on the surface and inside the metal	Only for ferromagnetic materials, and only surface and near-surface defects can be found.
Ultrasonic	Can detect surface and internal defects of various objects	Need coupling agent, strict requirements for workpiece, such as surface finish, etc.
Laser scanning	High sensitivity, real-time, can detect surface information in three dimensions	Low resolving power, low maintainability and adaptability
Machine Vision	Simple system structure, strong adaptability, high accuracy, good detection real-time	The imaging environment is different and there are many factors to consider

The heavy rail under the hot condition is characterized by high temperature surface texture distribution. Different parts of the section have different infrared radiation capabilities, complex three-dimensional contours, rough and obvious surface texture, fast rolling speed, many types of defects, large amount of data, and high requirements for real-time detection. Therefore, this high-temperature textured curved steel members are different from normal temperature objects, whose strong infrared radiation, surface noise and glare make conventional detection methods ineffective, while visual inspection creates conditions for its application in the field of high-temperature defects detection due to its unique advantages.

However, in the hot heavy rail environment, it is impossible or difficult to observe directly with the naked eye, therefore, machine vision inspection is used to work in high temperature and high thermal radiation environment, which can continuously collect images of the surface of the heavy rail in the process and can realize seamless imaging of all sides of the heavy rail. The use of a stable database and communication method makes the preservation cycle of the detection object larger, the analysis results more accurate, and the information call more convenient. Finally, it makes the defects detection on the surface of heavy rail reach a high level of automation intelligence.

The surface profile of the hot heavy rail is complex, with infrared radiation, and vulnerable to multiple noise interference factors such as illumination, viewing angle, water vapor, and power fluctuation. Therefore, it is necessary to study the fusion of multi CCD(Charge Couple Device) for full-image acquisition of hot heavy rail, consider the influence of the coupling degree between multiple parameters on the imaging quality, and continuously acquire images of the surface of heavy rail in the process to achieve clear images of each surface[15].

2. SURFACE CHARACTERISTICS OF THE HEAVY RAIL

The cross section of the heavy rail is shown in Figure 2, the surface of the heavy rail is with multiple planes and multiple surfaces. Heavy rail specification size and its nominal weight has a relationship, but the shape is roughly the same, its specific size can be obtained from TB/T 2344 and other relevant standards, the size shown in the figure for the nominal weight of 60Kg/m specification of heavy rail.

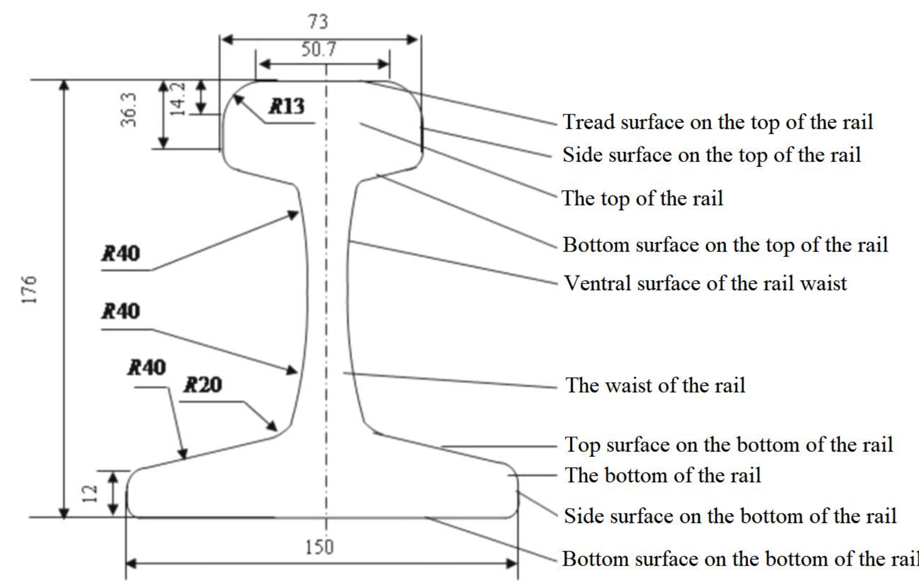

Figure 2. 60Kg/m heavy rail size and shape characteristics

The heavy rail is divided into three parts, the top of the rail , the waist of the rail and the bottom of the rail. From the full surface of the heavy rail, there are several curved surfaces and flat surfaces. The plane includes tread on the top of the rail, side on the top of the rail, slide on the bottom of the rail, and bottom on the bottom of the rail, etc.

3. THE GENERAL STRUCTURE OF THE VISION INSPECTION SYSTEM

Inspection system is mainly composed of line array CCD, network module(network cable, fiber optic, photoelectric conversion module), frame grabber (FG) and computer storage and processing system, etc. CCD will receive the heavy rail surface information into image signal output to image acquisition card, image acquisition card and then convert the signal into digital image information for computer processing and display, the computer uses a variety of algorithms to image data processing operations, calculate the detected Whether there are defects on the surface of the heavy rail [16-19].

Under the condition of dark field illumination detection light path, multiple high-speed line array cameras are used for image acquisition on the whole surface of the heavy rail, and multiple images are output to the image acquisition card through 1000Mbits super 6 network cable in parallel to realize the long-distance stable transmission of image data, and the image acquisition card then converts the signal into digital image information for computer processing and display, and the computer uses various algorithms to process and calculate the image data to complete the calculation of the defects on the surface of the heavy rail. The computer uses various algorithms to process the image data to complete the task of detecting and identifying the defects on the surface of heavy rail. The principle of the detection system is shown in Figure 3.

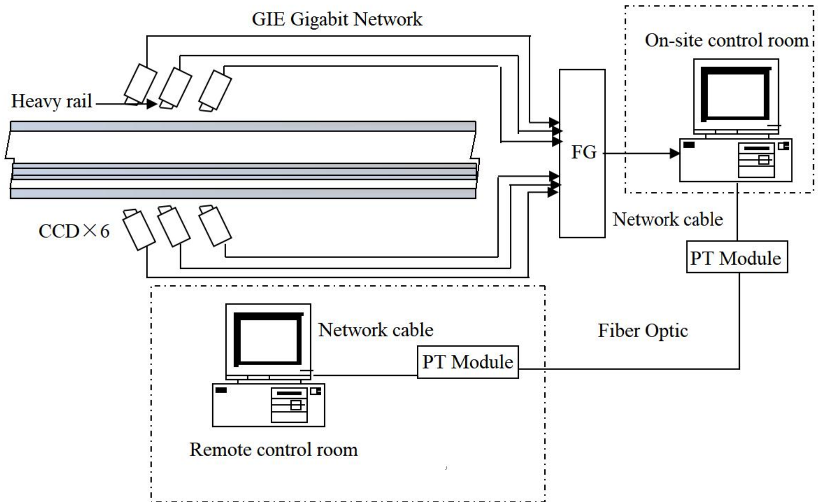

Figure 3. Composition of the vision system for heavy rail defects detection

As shown in Figure 4, a total of six CCD cameras line scan six parts of the heavy rail from six angles, and the cameras take pictures of the tread, bottom, upper waist and lower waist of the rail respectively. Basically cover the whole surface area of the heavy rail. Each camera each camera corresponds to a set of support frame, the frame multi-degree of freedom adjustable, to ensure that can meet a wide range of changing object distance and shooting angle requirements. Camera 1 and camera 2 correspond to the top shelf 1 and top shelf 2 respectively; camera 3 and camera 6 correspond to the side shelf 3 and side shelf 6; camera 4 and camera 5 correspond to the bottom shelf 4 and bottom shelf 5.

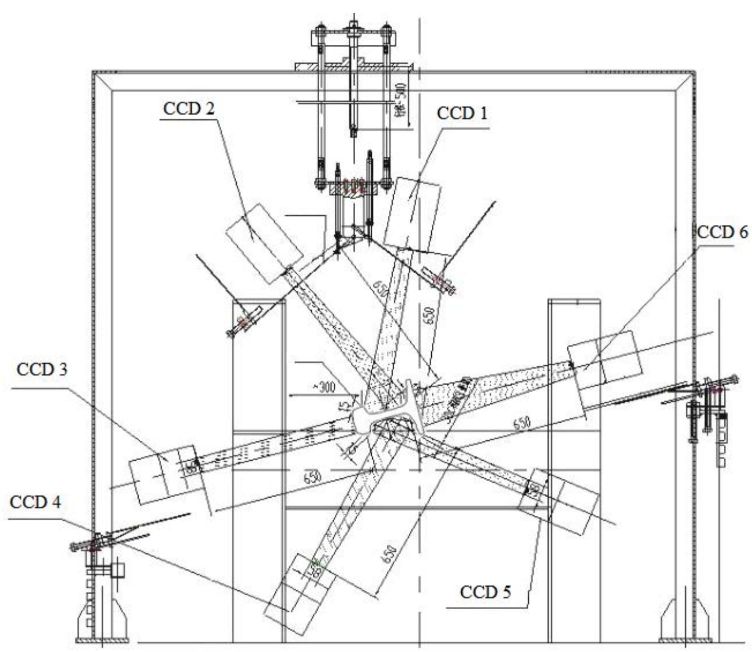

Figure 4. Distribution of the camera

1,2 The acquisition unit is positioned above the heavy rail and its mechanism is mounted on the gantry beam that spans the top of the heavy rail line. In the acquisition unit, the camera is mounted inside the guard, which is fixed to the mechanism by the head. By adjusting the mechanical device, the acquisition unit can realize the movement in three directions and change the camera position to meet the requirements of focus and shooting angle change. 1, 2 acquisition unit is directly above the heavy rail, and there is no isolation in the middle, due to the thermal radiation of the heavy rail, the temperature above it is very high, so the heat insulation baffle is added between the acquisition unit and the heavy rail, the lower surface of the baffle is coated with anti-radiation paint, and the baffle has a certain size of slot on it. The camera can take pictures of the heavy rail through the slot.

At the location of UF of heavy rail production line, multiple image sensors are set up, and the collected image data are converted into digital images through A/D, and the digital images enter the central processing server through gigabit network cable, and the data processed by the central processing computer enter the database storage. Each client can be used for online or offline image observation and data analysis at any time, and various information will be managed at the same time. The system integrates acquisition, transmission, processing, management and service, and provides external interfaces for remote data communication or analysis.

3.1 Line scan imaging analysis

Conventional surface-scanning camera acquires a number of lines of images at a time, while the line array camera usually has only one line of light-sensitive units, each acquisition of one line of images, each output line of images, the CCD sensor will convert the light energy into a video pulse signal, the video signal is then converted into a digital signal output by the A/D circuit. Rail surface line scan imaging principle is a line array CCD along the direction perpendicular to the movement of the heavy rail to scan out N lines of images [20-21]. If the acquisition frequency is set appropriately, these N lines of images will be seamlessly stitched into the heavy rail surface image, As Shown in Figure 5.

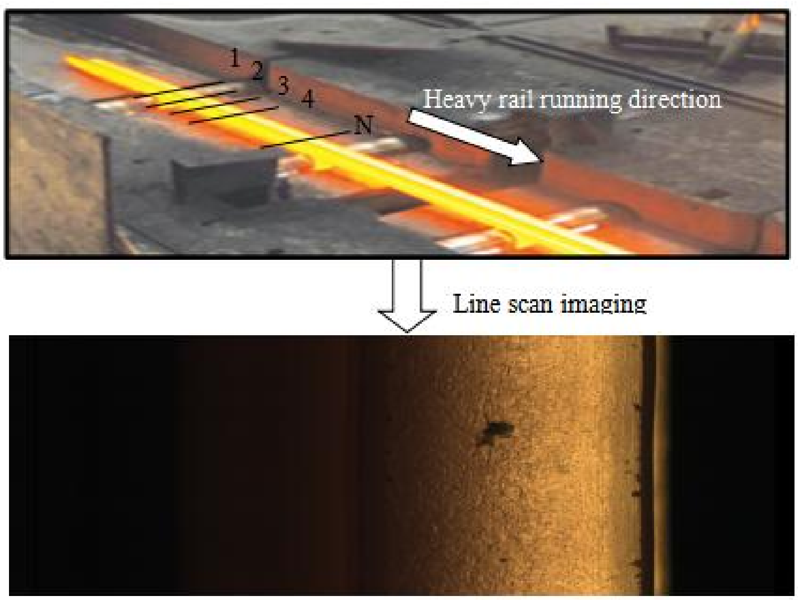

Figure 5. Principle of line scan for heavy rail

Calculation of heavy rail tread imaging. Field of view = image element size × number of pixels × working distance / focal length, if the line array camera CCD image element size of 14 μ s, the number of pixels for the case of 1024, according to Figure 5, we can determine the focal length: f = wL / W, where w = 1024 × 14 μ s, increase the focal length can reduce the field of view, so that the effective area of the picture occupies more pixels, the shooting target (heavy rail surface) will be more obvious, i.e., reduce the field of view and increase the accuracy of the display.

3.2 Acquisition synchronization analysis

Line array CCD synchronization includes two parts: synchronization of single camera line scan frequency with the motion speed of the subject; frame synchronization of multiple cameras.

(1) Synchronization of line scan frequency and motion speed

In order to protect the camera and minimize the influence of infrared radiation on the imaging, the camera must be far enough from the heavy rail, but the distance should not be too large, otherwise it may lead to too much background being taken into the field of view, resulting in a lower lateral resolution of the heavy rail. The DALSA line array CCD used in the system, its image element size is 14 μ s, the lateral resolution is 2048, to illustrate the imaging of heavy rail tread as an example, 60kg/m of heavy rail tread width is 73mm, rolling speed fluctuates up and down in 3m/s. Because the rolling process there is lateral jitter, the field of view width of 120mm is more appropriate, the object distance is selected 300mm. then the image distance (mm) = 71.68mm. then according to $1/u + 1/v = 1/f$ imaging formula, the focal length can be calculated about 58mm, as the basis for the optional lens. The transverse resolution of the heavy rail is about 0.06mm. the maximum line frequency of the camera is 18KHz. the initial stage of rolling, the running speed of the heavy rail is low, and as the rolling proceeds, the speed may increase to 1000mm/s. at this moment, the highest longitudinal accuracy of this line array CCD in shooting is 1000(mm/s)/ 18000Hz = 0.055mm, which meets the requirement. In order to make the scanning frequency of the acquisition system change with the change of the moving speed of the subject, the encoder can be considered to generate the motion speed code of the target to generate the camera line trigger signal, each rotation of the motor, the corresponding encoder output N pulses, the pulse count of the encoder in the unit time, you can calculate the motor speed, speed changes, line scan frequency changes accordingly, the acquisition frequency and the subject The current accuracy of the camera is the essence of the camera is to let the camera's current work line frequency along with the speed of the shooting object changes, when the object movement speed increases the camera's work line frequency also increases accordingly, when the object movement speed decreases the camera also increases accordingly, when the object movement speed decreases the camera line frequency also decreases at the same time, but the ratio of the two, that is, the accuracy always remain constant.

(2) Multi-camera acquisition synchronization

The system, heavy rail full surface image by 6 CCD synchronous real-time acquisition, if a color image resolution of 2048 × 2048, pixel bit depth of 32bit, frame rate of 2 frames / second, the amount of data generated by 6 CCD per second is 192MB. Therefore, when the CCD full resolution work When the storage system burden is quite large, you can consider the introduction of SCSI-RAID technology and capture card BMP original picture into JPG compressed picture technology to solve the data storage bottleneck, the former by several SCSI hard disk in the form of a daisy chain to form a RAID storage system to achieve cross-recording, each SCSI hard disk has enough cache to make the total storage speed close to SCSI interface speed, thereby increasing the bandwidth of the storage system. The clock signal of one CCD is used to synchronize the other cameras to achieve synchronous acquisition of 6 CCD. CCD 1 uses the internal pulse generator to generate the clock signal, and while providing itself as the reference, the signal is output to the other 5 CCD through GPIO (programmable IO), and the other 5 CCD are set to the external synchronization mode, and during the image acquisition process, the 6 CCD use The clock signal generated by the pulse generator of CCD 1 is used as the reference for synchronous acquisition.

3.3 Lighting analysis of the light source

The heavy rail surface defects detection system, the use of a line CCD camera, compared to the surface CCD, its scanning frequency is very block, the exposure time is very short, the heavy rail surface of the high temperature radiation light through the filter to the camera light is extremely limited, the line CCD failed to fully sense the radiation light, resulting in the image of the heavy rail surface and background distinction is not obvious, defects and iron oxide can not be distinguished, the overall contrast is low. Therefore, the dark domain imaging was carried out by halogen lamp light source, and the imaging effect with and without light source is shown in Figure 6. a below. It is found that the image quality is greatly improved, and the distinction between the surface of the heavy rail and the defects is more obvious, and the gray level of the defects or iron oxide is more abundant. It is further found that the heavy rail is at high temperature and radiates strong infrared light by itself, which can easily produce image brightness saturation as shown in Figure 6 b. By choosing the appropriate camera parameters and light source parameters, the effect of Figure 6. c can be obtained.

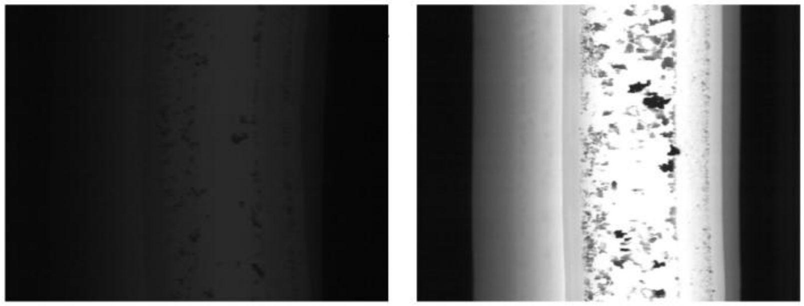

(a) no light source and the effect of light source comparison

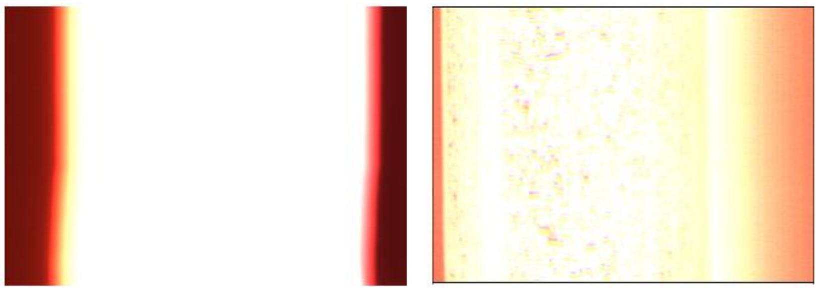

(b) Imaging with light source, overexposed

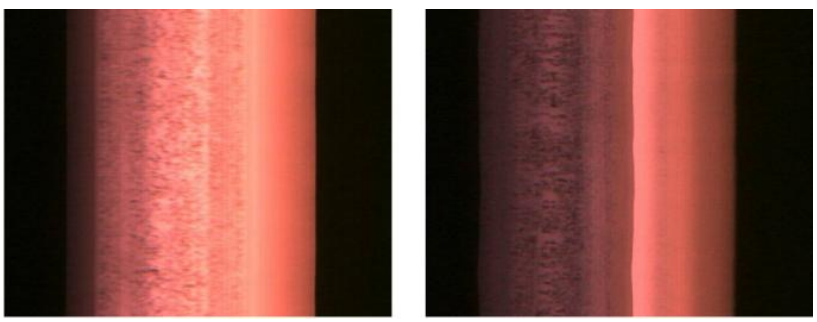

(c) Imaging with light source, normal exposure, no filter

Figure 6. Surface imaging under different conditions

However, the imaging effect of Fig. 6(c) still cannot distinguish the background and defects well, which is due to the high-temperature thermal radiation of the heavy rail, and some invisible light band radiation affects the imaging quality and must be filtered out. Therefore, by matching the spectral sensitivity response curve of the CCD with the wavelength range of the light source, a suitable filter is selected to filter out the stray light of non-light source wavelengths. As shown in Figure 7, the shooting effect of QB21 glass filter (left) and GRB3 glass filter (right) are shown respectively.

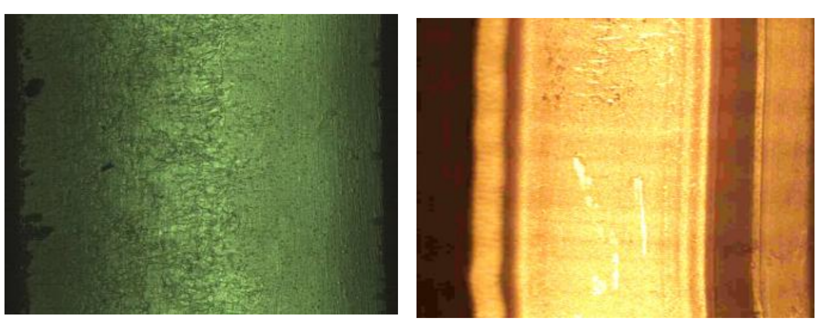

Figure 7. Different through-lighting curve and shooting effect

In summary, choose to add a filter in front of the lens to filter out some interference bands of light, the image quality improved significantly.

4. IMAGE CLARITY EVALUATION EXPERIMENT

The main research on two aspects to obtain clear and interference-free images of the heavy rail surface. First, to obtain a clear and stable image of the heavy rail surface. Through the focus evaluation function, the focus of the camera is adaptively adjusted to reduce the blurring of the image due to the vibration effect during the rolling of the heavy rail. Secondly, by analyzing the causes of the formation of uneven illumination phenomenon, the corresponding solutions are proposed, and finally the image quality is evaluated by the image quality evaluation function to lay a good foundation for the next step of defects pattern classification work.

Ten images of heavy rail surface labeled "U75V" with a resolution of 176×344 and a total of 59856 pixels were selected. As shown in Figure 8, it can be seen that the images went through the process of "out of focus - focus - out of focus", i.e., the images gradually became clear from the initial blurred stage, and slowly became blurred again. The focus of the 6th and 7th images is significantly better than the other images, and it can be judged that the images at this stage belong to the focus stage.

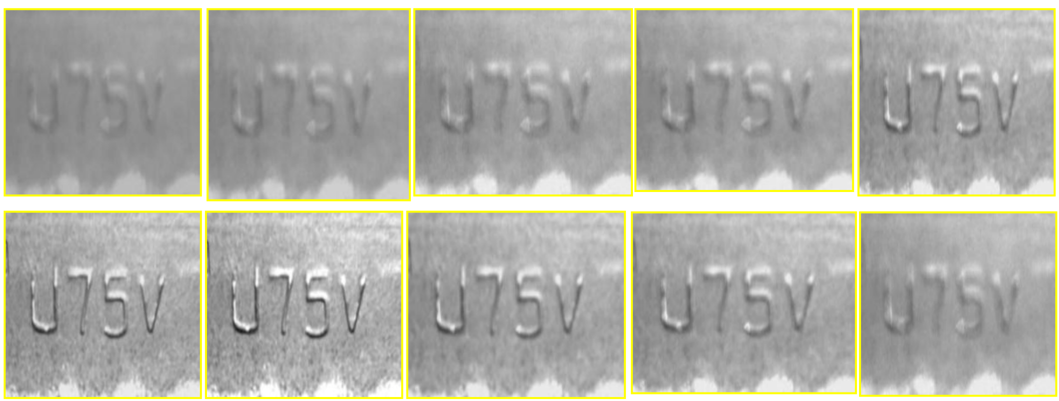

Figure 8 "Out of focus - focus - out of focus" process of heavy rail mark "U75V

These 10 images were subjected to the grayscale difference operation, and the histogram changes of grayscale between each gradient were counted, and the differences between the gradient histograms of out-of-focus and focused images were compared, and the number of pixels with different gradient values for the 10 images of "out-of-focus-focus-out-of-focus" were calculated, and the statistics were obtained as shown in Table 2.

Table 2. pixel number of each grads in different image

Gradient level	**Image**									
	1	**2**	**3**	**4**	**5**	**6**	**7**	**8**	**9**	**10**
0.5~1	25049	18946	10858	11226	9668	6224	5543	7213	9331	10858
1~2	19855	21726	20433	20488	16073	6196	4026	14636	16095	20433
2~3	5611	8596	12097	12054	14017	8696	6224	13666	14217	12097
3~5	3732	5317	7933	8040	12250	17090	14247	13681	12171	7933
5~8	678	2173	3709	3582	4889	14277	16300	5250	4715	3709
8~12	13	215	1137	1225	2644	6142	9276	2805	2634	1137
12~20	0	2	63	78	1446	3330	4675	2017	1431	63
20~30	0	0	0	0	172	1332	1765	496	164	0
30~40	0	0	0	0	3	501	757	73	3	0
>40	0	0	0	0	0	228	543	5	0	0

As can be seen from Table 2, for the out-of-focus images (Figures 1~5, Figures 8~9), the peak number of pixels of the images appears in the range of thresholds 0.5~1 and 1~2, and the peak value of each image does not differ much, and in the other threshold ranges, the number of pixels is gradually less with the increase of thresholds, and the value is 0 beyond a certain threshold range; for the focused images (Figures 6~7), the peak number of pixels purpose appears in the between gradient levels 3 and 8, and the number of pixels within the threshold at each level is distributed more uniformly and smoothly, and when the gradient value is greater than 20, the number of pixels in the clear focused image is significantly larger than that in the blurred out-of-focus image. Therefore, according to the statistical law, focus adjustment can be performed to obtain clear images, and the results can be fed back to the camera to achieve automatic focus during image acquisition. Increase the contrast between the defective and background areas of the image.

5. CONCLUSION

The paper analyzes and summarizes the characteristics of various NDT, proposes a machine vision-based inspection scheme for the characteristics of heavy rail surface with variable shape and complex cross-sectional profile, which is connected by multiple planes and multiple curved arcs, and designs the overall structure of the heavy rail surface defects detection system, and proposes a specific implementation scheme for each module with the goal of modularizing the system's hardware construction and software functions The system is modularized in terms of hardware construction and software functions. Six line array CCD are used to photograph the tread surface, bottom surface, upper waist surface and lower waist surface of the heavy rail. In order to solve the illumination problem when the line array CCD is moving at high speed, a comprehensive comparison of various types of light sources is made through chromaticity, brightness, spectral power theory and experimental effects. And through the statistical method to realize the automatic focus in the image acquisition process, to ensure the clear acquisition of multi-surface images of the hot heavy rail, and lay a good foundation for further defects classification.

ACKNOWLEDGEMENTS

This research was funded by the National Natural Science Foundation of China , grant number 61901068, and the Chongqing Natural Science Foundation, grant number cstc2021jcyj-msxmX0525, and the Sci. & Tech Foundation of CMEC, grant number KJQN201901150, KJQN202001131.

REFERENCES

[1] Wu, Y., Lee, C. C., Lee, C. C., Peng, D., Geographic proximity and corporate investment efficiency: evidence from high-speed rail construction in China. Journal of Banking & Finance, 140, 106510 (2022).

[2] Li, Z. W., Liu, X. Z., Yang, F., Zhang, L. W., Mud Pumping Defect Detection of High-Speed Rail Slab Track Based on Track Geometry Data [J]. Journal of Transportation Engineering, Part A. Systems, 148(6), 04022023 (2022).

[3] Tang, M., Sun, H., China’s High-Speed Railway Development History. In High-Speed Rail: An Analysis of the Chinese Innovation System, pp. 385-424 (2020).

[4] Xie, Z. J., Mi, Z. Z., Chen, T., et al., Surface defect inspection technique for hot heavy rail[J]. Jiliang Xuebao/Acta Metrologica Sinica, 34(1):1-6 (2013).

[5] Xie, C., Xu, H., Liu, Y., et al., Hot-Rolled, Heavy-Rail Image Recognition Based on Deep-Learning Network[J]. Journal of web engineering, (5):1623-1640 (2021).

[6] Albano, C., Camacho, N., Reyes, J, et al., Influence of scrap rubber addition to Portland I concrete composites: Destructive and non-destructive testing[J]. Composite Structures, 71(3/4):439-446 (2005).

[7] Usamentiaga, R., Venegas, P., Guerediaga, J., et al., Infrared Thermography for Temperature Measurement and Non-Destructive Testing[J]. Sensors, 14(7):12305-12348 (2014).

[8] Zec, M., Uhlig, R. P., Ziolkowski, M., et al., Fast Technique for Lorentz Force Calculations in Non-Destructive Testing Applications[J]. IEEE Transactions on Magnetics, 50(2):133-136 (2014).

[9] Li, Z., Meng, Z., A Review of the Radio Frequency Non-destructive Testing for Carbon-fibre Composites[J]. Measurement Science Review, 16(2),68-76 (2016).
[10] Yang, J., Defect Detection inside a Rail Head by Ultrasonic Guided Waves[J]. Symmetry, 14(12):2566 (2022).
[11] Kang, H., Min, S., Seo, B., Roh, C., Hong, S., Cheong, J. H., Preliminary studies of perovskite-loaded plastic scintillator prototypes for radioactive strontium detection. Chemosensors, 9(3), 53 (2021).
[12] Hughes, R., Dixon, S., Developments in near electrical resonance signal enhancement (NERSE) eddy-current methods[J]. American Institute of Physics, 1650:345-352 (2015).
[13] Rifai, D., Abdalla, A. N., Ali, K., Razali, R., Giant magnetoresistance sensors: A review on structures and non-destructive eddy current testing applications. Sensors, 16(3), 298 (2016).
[14] Finkle, L. J., Hybrid Induction Eddy Current Ring Motor with Self Aligning Hybrid Induction/Permanent Magnet Rotor: U.S. Patent Application 17/307,712[P]. 2021-8-19 (2021).
[15] Finantu-Dinu, E. G., Korzec, D., Engemann, J., Investigation of the surface barrier discharge topology by use of intensified CCD camera. In Proc. of XXVI Int. Conf. on Phenomena in Ionized Gases ICPIG 2003, vol 4, pp. 61-2 (2003).
[16] Zhou, L., Chalana, V., Kim, Y., PC-based machine vision system for real-time computer-aided potato inspection[J]. International Journal of Imaging Systems & Technology, 9(6):423-433 (2015).
[17] Baigvand, M., Banakar, A., Minaei, S., Khodaei, J., Behroozi-Khazaei, N., Machine vision system for grading of dried figs[J]. Computers & Electronics in Agriculture, 119(C):158-165 (2015).
[18] Ding, Y., Zhang, X., Kovacevic, R., A laser-based machine vision measurement system for laser forming[J]. Measurement, 82:345-354 (2016).
[19] Ardhy, F., Hariadi, F. I., Development of SBC based machine-vision system for PCB board assembly automatic optical inspection. In 2016 International Symposium on Electronics and Smart Devices (ISESD) (pp. 386-393). IEEE (2016).
[20] Zhang, L., Xie, K., Li, T., Based on line scan CCD print image detection system. In MIPPR 2015: Pattern Recognition and Computer Vision (Vol. 9813, pp. 174-180). SPIE (2015).
[21] Shrestha, P., Barbieri, M., Weda, H., et al., Synchronization of Multiple Camera Videos Using Audio-Visual Features[J]. IEEE Transactions on Multimedia, 12(1):79-92 (2010).